Calculated lifetimes of hot electrons in aluminum and copper using a plane-wave basis set

Wolf-Dieter Schöne, Robert Keyling, Mario Bandić, and Walter Ekardt

Fritz-Haber-Institut der Max-Planck-Gesellschaft, Faradayweg 4-6, 14195 Berlin, Germany

We report about the lifetimes of hot electrons in crystalline aluminum and copper. For aluminum the results agree quantitatively with the experimental results. For copper we get good agreement for quasiparticle energies in the (110) direction above 2 eV which shows that the lifetimes for quasiparticle states above 2 eV are determined by sp bands, explaining the puzzling fact that simple Fermi liquid theory describes Cu in this direction quite well. The calculations were performed within the shielded interaction approximation using a plane-wave basis expansion for the wave functions. We show that for Cu this basis leads to equally good results as the more demanding linearized augmented plane-wave basis. [S0163-1829(99)10835-X]

I. INTRODUCTION

The understanding of the physical and chemical reactions on surfaces on a microscopic level is one of the major goals in modern surface physics. A very interesting subfield is the understanding—and possible future engineering—of photo-chemical processes on surfaces. As one step in this direction the study of the lifetime of excited electrons is currently a very active field.

Copper has been one of the first elements for which the lifetime of excited electrons has been measured using modern time-resolved two-photon photoemission spectroscopy (TR-2PPE).[1–7] In these experiments electrons from the valence band are excited by a femto-second laser pulse (the so-called pump laser) into the conduction band. A second (time-delayed) photon excites the electron above the vacuum level where it can be detected. By varying the time delay between the two laser pulses this technology allows the measurement of the lifetime of electrons in excited states.

The measured lifetime of excited electrons is determined by several distinct physical processes. The most important is electronic correlation. The second contribution is transport away from the surface. The experiments are typically conducted about 30 Å to 50 Å below the surface.[7] Drifting of an excited electron into the bulk—before the probe laser can eject it—will lead to a measured lifetime which is shorter than the actual lifetime. A third process which has to be considered is the so-called cascading.[7] The excited electron leaves a hole in the valence band. Particle and hole may recombine and excite another electron via an Auger process. This process leads to measured lifetimes which are too long. Connected to this is another observation: in some systems, such as, e.g., copper, where it has been observed first by Pawlik, Bauer, and Aeschlimann,[5] the lifetime of an excited electron at a fixed energy $E - E_F$ (E_F being the Fermi energy) depends on the frequency of the pump laser, i.e., the band from which the electron originated.

In order to extract valuable information about excited electrons from the experiments it is important to disentangle these processes by understanding each of them. In the following we are considering the first process, namely, the intrinsic lifetime of excited quasiparticle states due to electronic correlation effects. It is the dominant process for determining the lifetimes and is up to now still treated within Fermi liquid theory (FLT).[8–10]

II. THEORY

We are dealing with an interacting many-electron system. So the natural starting point for our calculations is a well-converged solution of the Kohn-Sham (KS) equations[11,12] within density functional theory (DFT),[13]

$$\left(-\frac{\hbar^2}{2m}\nabla^2 + v_{\text{eff}}(\mathbf{r}) \right)\varphi_{\mathbf{q},j}(\mathbf{r}) = \epsilon_{\mathbf{q},j}\varphi_{\mathbf{q},j}(\mathbf{r}). \tag{1}$$

$\mathbf{q}$ and j denote a wave vector in the Brillouin zone (BZ) and a band index, respectively. $v_{\text{eff}}(\mathbf{r})$ is the mean-field potential in which the KS electrons move. It is given by

$$v_{\text{eff}}(\mathbf{r}) = v_{\text{ion}}(\mathbf{r}) + v_{\text{coul}}(\mathbf{r}) + v_{\text{xc}}(\mathbf{r}). \tag{2}$$

Here v_{ion} is the crystal potential set up by the ionic cores. In our *ab initio* treatment it is considered exactly, either by doing an all-electron calculation or by applying norm-conserving pseudopotentials. v_{coul} is the classical Coulomb potential (Hartree potential) and v_{xc} the so-called exchange-correlation potential. It contains all quantum-mechanical contributions to the electron-electron interaction. In real calculations it is approximated using local density approximation (LDA).[12] However, the KS equations describe only ground-state properties, i.e., they are not suitable for calculating the properties of *excited* states. Moreover, since the Hamiltonian in Eq. (1) is Hermitian the eigenvalues $\epsilon_{\mathbf{q},j}$ are real. Any lifetimes calculated within this framework are therefore infinite. In order to describe properly the dynamical processes one has to go back to many-body perturbation theory (MBPT).[14]

Within MBPT the dynamics of a many-particle system is described by the Dyson equation[15]

$$\left(-\frac{\hbar^2}{2m}\nabla^2 + v_{\text{eff}}(\mathbf{r}) \right)\psi_{\mathbf{q},j}(\mathbf{r}) + \int d^3r' \tilde{\Sigma}(\mathbf{r},\mathbf{r}';E_{\mathbf{q},j})\psi_{\mathbf{q},j}(\mathbf{r}')$$

$$= E_{\mathbf{q},j}\psi_{\mathbf{q},j}(\mathbf{r}). \tag{3}$$

Compared to the KS equations it contains an additional ''potential term'' which is non-local, complex, and energy de-

pendent. Instead of the real eigenvalues $\epsilon_{\mathbf{q},j}$ its solutions are complex quasiparticle energies $E_{\mathbf{q},j}$. Therefore the time evolution of the system is no longer oscillatory but contains an additional decaying term which defines the lifetime of the quasiparticle state[16]

$$e^{i\epsilon t/\hbar} \rightarrow e^{(i[\epsilon - \mathrm{Re}\{\Sigma\}]t/\hbar)} e^{(-\mathrm{Im}\{\Sigma\}t/\hbar)}, \qquad (4)$$

where $\mathrm{Re}\{E\} = \epsilon - \mathrm{Re}\{\Sigma\}$ and $\mathrm{Im}\{E\} = -\mathrm{Im}\{\Sigma\}$ are the real and imaginary part of the quasiparticle energy E, respectively. Σ is the electronic self-energy.

In practice the Dyson equation is solved within a certain basis set. We use the Bloch basis, i.e., the orthonormal set of solutions of the KS equations [Eq. (1)], for a crystalline system.[17,18] Furthermore, we work on the imaginary frequency axis (Matsubara axis). The Dyson equation can then be transformed from the form of Eq. (3) into

$$G_{j,j'}^{-1}(\mathbf{q}, i\omega_m) = G_{j,j'}^{\mathrm{LDA}-1}(\mathbf{q}, i\omega_m) - \tilde{\Sigma}_{j,j'}(\mathbf{q}, i\omega_m), \qquad (5)$$

where $\mathbf{q}$ is a vector in the BZ, j, j' are band indices, and the ω_m are fermion Matsubara frequencies, $\omega_m = \pi(2m+1)/(\beta\hbar)$. $G_{j,j'}(\mathbf{q}, i\omega_m)$ is the dressed Green's function and $G_{j,j'}^{\mathrm{LDA}}(\mathbf{q}, i\omega_m)$ the propagator of the KS electrons,

$$G_{j,j'}^{\mathrm{LDA}}(\mathbf{q}, i\omega_m) = \frac{\delta_{j,j'}}{i\omega_m - \omega_{\mathbf{q},j}}. \qquad (6)$$

The $\omega_{\mathbf{q},j}$ are the KS eigenvalues measured from the chemical potential μ, $\hbar\omega_{\mathbf{q},j} = \epsilon_{\mathbf{q},j} - \mu$. A detailed description of this method can be found in Refs. 18,19.

We calculate the self-energy within the shielded interaction approximation (SIA or GW approximation),[8,15,20–22] in which Σ is given as the product of G^{LDA} and the shielded potential V^S,

$$\Sigma^{\mathrm{xc}}(\mathbf{r}, \mathbf{r}'; t) = iG_{\mathrm{LDA}}(\mathbf{r}, \mathbf{r}'; t)V_S(\mathbf{r}, \mathbf{r}'; t^+). \qquad (7)$$

The shielded potential is just the bare Coulomb potential v screened by the dielectric function, $V_S = v/\epsilon$. It is obtained from the polarizability P by solving a matrix equation in the band indices[18] for each wave vector $\mathbf{q}$ and each frequency $i\omega_m$. In the Bloch basis Eq. (7) becomes

$$\Sigma_{j,j'}^{\mathrm{xc}}(\mathbf{q}, i\omega_m) = -\sum_{\mathbf{k}}^{\mathrm{BZ}} \sum_{\mu,\nu,\mu',\nu'} A_{\mu,j,\mu'}^*(\mathbf{q}-\mathbf{k}, \mathbf{q}, \mathbf{k})$$

$$\times A_{\nu,j',\nu'}(\mathbf{q}-\mathbf{k}, \mathbf{q}, \mathbf{k})$$

$$\times \frac{1}{\beta\hbar} \sum_{i\omega_n} G_{\mu',\nu'}^{\mathrm{LDA}}(\mathbf{k}, i\omega_n)$$

$$\times V_{\mu,\nu}^S(\mathbf{q}-\mathbf{k}, i\omega_m - i\omega_n). \qquad (8)$$

$\mathbf{k}$ and $\mathbf{q}$ are elements of the BZ and the irreducible Brillouin zone (IBZ), respectively. $\mathbf{k}-\mathbf{q}$ is understood to be folded back into the BZ. The coefficients A are defined as the integrals of three Bloch functions

$$A_{j,\mu,\nu}(\mathbf{q}, \mathbf{k}+\mathbf{q}, \mathbf{k}) = \int d^3r \, \psi_{\mathbf{q},j}^*(\mathbf{r}) \psi_{\mathbf{q}+\mathbf{k},\mu}(\mathbf{r}) \psi_{\mathbf{k},\nu}^*(\mathbf{r}). \qquad (9)$$

Once the self-energy has been calculated the Dyson equation (5) can be solved. In order not to account for exchange and

correlation effects in the Dyson equation twice, the self-energy has to be corrected by those contributions already considered in v_{xc}, $\tilde{\Sigma}^{\mathrm{xc}} = \Sigma^{\mathrm{xc}} - v_{\mathrm{xc}}$. Furthermore, the new chemical potential has to be determined. (Within the LDA the Fermi energy equals the chemical potential.[12,19] In the quasiparticle picture the term Fermi energy is no longer defined because of the renormalization of the Fermi function. Nevertheless we will use the term Fermi energy in the following meaning the chemical potential.) Having obtained the Green's function on the Matsubara axis we can now perform an analytic continuation using standard Padé approximation techniques[23,24] to obtain the retarded Green's function $G_{j,j'}(\mathbf{q}, \omega)$. The spectral function is defined by

$$A_{j,j'}(\mathbf{q}, \omega) = -2 \, \mathrm{Im} \, G_{j,j'}(\mathbf{q}, \omega). \qquad (10)$$

It contains complete information about the one-particle properties, especially the real and imaginary parts of the quasiparticle energies.[25] The spectral function is calculated for all wave vectors in the Brillouin zone and all bands. From $A_{j=j'}(\mathbf{q}, \omega)$ the width of the quasiparticle excitation $\Delta_{\mathbf{q},j}$ is extracted. In order to obtain data which are dense enough to be compared to experiment we perform a three dimensional interpolation of $\Delta_{\mathbf{q},j}$ in $\mathbf{k}$ space. The lifetime is simply[14] $\tau_{\mathbf{q},j} = 1/\Delta_{\mathbf{q},j}$.

The SIA forms a set of equations which have to be solved self-consistently.[15,20–22] However, it has been shown by several authors[18,25–29] that self-consistent calculations lead to results which compare much less with experiment than calculations in which the self-energy is evaluated only once. In the latter case typically very good agreement with experiment is achieved.[22,30–32] Two examples where this is illustrated very clearly are the occupied bandwidth in simple metals and the fundamental band gap in silicon. Whereas in LDA calculations the occupied bandwidth in simple metals is too large and the band gap in semiconductors much too small, a GW calculation in which the self-energy is calculated only once leads to values for the occupied bandwidth and the band gap in semiconductors which are typically within 10% of the experimental values.[30,32,33] If the Dyson equation is solved self-consistently this agreement is destroyed. In fact the self-consistent results disagree more with experiment than results from conventional LDA calculations.[18,25–27] It seems that if the self-energy is evaluated only once a cancellation of errors occurs which is not present in the case of self-consistency. In other words, the physics underlying the GW approximation describes the electronic correlation incorrectly. Additional diagrams need to be included. So at present the situation is as follows; the SIA or GW approximation leads to very good results if done non-self-consistently although it is not fully understood why. If one wants to perform realistic calculations beyond the LDA level it is the method which has to be used.

We close this section with a couple of technical remarks. On the level of the first evaluation of the self-energy the Hartree part of the self-energy (tadpole diagram) equals the Hartree potential of the KS equations. Since we calculate the self-energy only once, it is therefore sufficient to determine only the exchange-correlation part of the self-energy $\Sigma_{j,j'}^{\mathrm{xc}}$. We only calculate the diagonal elements ($j=j'$) of the self-energy since it has been shown that the off-diagonal ele-
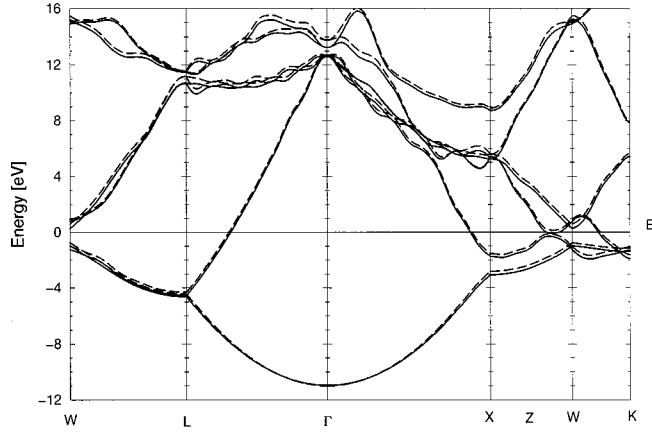
FIG. 1. The LDA band structure of Al (dashed line) compared to the quasiparticle band structure (solid line). As expected for an element with a small Wigner-Seitz radius the difference is rather small.

ments can be neglected.[30,34] It is, however, crucial to consider the full matrix of the shielded potential $V_{j,j'}^{S}(\mathbf{q},i\omega_n)$ when determining the self-energy.[18,28] Calculating the self-energy only once has another consequence. The polarizability is the product of two Green's functions,[25] $P=GG$. In the case that $G=G^{LDA}$ the frequency summation can be done analytically, leading to the familiar form

$$P_{j,j'}(\mathbf{q},i\omega_n) = \frac{2}{V}\sum_{\mathbf{k}}^{BZ}\sum_{\mu,\nu}\frac{f_{\mathbf{k},\mu}-f_{\mathbf{k+q},\nu}}{i\omega_n+\omega_{\mathbf{k},\mu}-\omega_{\mathbf{k+q},\nu}}$$
$$\times A_{j,\nu,\mu}(\mathbf{q},\mathbf{k+q},\mathbf{k})A_{j',\nu,\mu}^{*}(\mathbf{q},\mathbf{k+q},\mathbf{k}).$$
$$(11)$$

III. THE LIFETIME OF ALUMINUM

The starting point for our discussion about the lifetimes of excited electrons in Al is the band structure as shown in Fig. 1. The dashed line denotes the LDA band structure,[35] the solid line the quasiparticle band structure. As can be seen from the figure the two curves differ only little, a consequence of the small Wigner-Seitz radius of Al ($r_s = 2.07$ eV). Al is one of the so-called nearly free-electron metals (NFE metals). Consequently the dominating part of the band structure is the sp bands along the directions Γ-L, Γ-X, and to a certain extent W-L. In the vicinity of the W point the band structure differs markedly from a free-electron system. The behavior of the band structure in W-L direction lies in between; it shows two nearly degenerate bands which are each sp-like. As will be shown below, this small deviation from the free-electron characteristic will lead to a striking difference between the real lifetime of excited electrons along this direction and the predictions from FLT. In FLT the lifetime is calculated for the homogeneous electron gas within the GW approximation. The dielectric function is approximated by a low frequency expansion. This leads to an expression for the lifetime in closed form,[8,10]

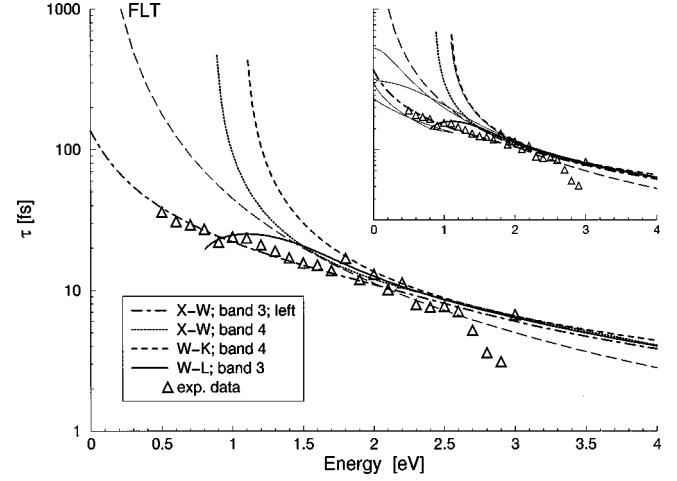$$\tau = \tau_0\frac{E_F}{(E-E_F)^2}, \qquad (12)$$

FIG. 2. The lifetime of excited electrons in Al plotted versus the energy of the electrons measured from the Fermi energy. The main part of the figure shows the bands and directions which we identified to be important for the explanation of the experimental data (Ref. 37). The most striking result is the lifetime of electrons in the third band in the W-L direction (solid line). At the band crossing of the third and fourth band around 1 eV (see Fig. 1) a new decay channel opens and the lifetime drops (see main text). The inset shows the lifetime of hot electrons in all directions and bands we have calculated. The denotation of the curves is the same as in the main part. The curves drawn with the thin solid lines are lifetimes of electrons in directions which were not probed by the experiment.

where the prefactor is given by

$$\tau_0 = \frac{64}{\pi^2}\sqrt{\frac{m}{3\pi ne^2}}. \qquad (13)$$

n is the density of the homogeneous electron gas. By construction Eq. (12) does not include any band-structure effects.

The lifetimes of excited electrons in Al were measured by Aeschlimann's group on a polycrystalline sample.[37] The frequency of the pump laser used in their experiment was 3.0 eV to 3.4 eV. For photons of this energy domain conservation of momentum allows only direct transitions. Inspection of the band structure in Fig. 1 shows immediately that only the low lying conduction bands in the W-X, W-K, and W-L directions can be populated by this pump laser and therefore only the lifetimes of electrons in these states were probed by the experiment.

Figure 2 shows the lifetimes of hot electrons in Al plotted versus the (quasiparticle) energy measured from the Fermi energy. The triangles denote the experimental results of Ref. 37. The long-dashed curve is the result of Eq. (12). The Wigner-Seitz radius of Al corresponds to $\tau_0 = 0.311$ fs. It does not explain the data very well, which is no surprise. As we argued above, the bands probed by the experiment of the Aeschlimann group have no free-electron-like character. The other four curves are our *ab initio* results for the selected directions and bands given in the legend. The most striking curve is the solid one. It displays the lifetime of electrons in the third band along the W-L direction. Starting from the L point and going down in energy as one approaches the W point the lifetime increases as predicted by FLT. Around 1 eV above the Fermi energy, the third band crosses the fourth

band. By this crossing interband transitions become possible and therefore an additional decay channel is opened. This results in a shorter lifetime, i.e., the curve bends down, in contrast to simple FLT. This explains the unusual behavior of the measured lifetimes around 1 eV. The remaining three curves show that the measured lifetimes originate from bands in the W-X and W-K directions and agree very well with the experimental data. Especially the (on first sight oscillatory) structure of the experimental data between 1.5 eV and 2 eV can be traced back to the lifetimes of excited electrons in two distinct bands. The sudden dropoff of three of the experimental data points beyond 2.5 eV cannot be explained by our data. We suspect that this dropoff is an artifact of the experimental setup.

The experimental data include all the processes mentioned in the Introduction whereas our calculation is restricted solely to electron-electron interaction. However, in Al transport effects play an important role. Therefore the authors of Ref. 37 corrected their measured lifetimes for transport effects according to Matthiessen's rule[37]

$$\frac{1}{\tau_{meas}} = \frac{1}{\tau_{ee}} + \frac{1}{\tau_{trans}}, \tag{14}$$

where τ_{meas} is the measured lifetime, τ_{ee} the lifetime due to electron-electron interactions, and τ_{trans} the lifetime correction due to transport effects, respectively. Bauer *et al.* used a value of $\tau_{trans} = 23$ fs. We corrected the measured lifetimes (the squares in Fig. 3 of Ref. 37) by $\tau_{trans} = 49.9$ fs. This difference in the transport corrections needs some explanations. Bauer *et al.* get the value of 23 fs from scaling the transport correction as obtained by a simple model calculation in Cu by the ratio of the Fermi velocities in copper and aluminum. Using 23 fs the experimental values coincide with the result of FLT (long-dashed curve in Fig. 2). FLT is a valid model to describe the effects of the sp bands in Al. However, as we argued above, due to momentum conservation the measured data are lifetimes of low lying states in the W-X, W-K, and W-L directions. These bands are definitely not sp-like. More serious is a point which is addressed already by the authors of Ref. 37; 23 fs seems to be a very

large transport contribution especially when compared with the data of the noble metals (note that the smaller τ_{trans} is, the larger is the transport effect). Furthermore, conductivity experiments suggest that the excited electrons of Al should be confined in a certain surface region[37] and therefore limiting the transport effects. In summary, it seems that a value of 23 fs is too small.

We obtained the value of $\tau_{trans} = 49.9$ fs by comparing our data with the experimental ones. So in this way we are even able to give a crude estimate for the size of the transport contributions to the overall lifetime. This approach is of course only possible for an element like Al, where electron-electron interaction and transport are the two largest contributions to the electronic lifetime. It also depends on the validity of Eq. (14). This validity has not been shown yet. Currently Eq. (14) is used due to the lack of a better—preferably *ab initio*—description of transport processes.

IV. COPPER

A. Ground state and polarizability

Cu is a noble metal with its $3d$ bands lying about 2–4 eV below the Fermi surface. The natural choice for a band-structure calculation is therefore a modern all-electron method such as, for example, the full-potential linearized augmented plane-wave (FP-LAPW) method[38] which has been coded, e.g., in WIEN95.[39] In the LAPW method the unit cell is divided up into nontouching spheres around the atoms with radius R_{MT} (denoted MT) and the remaining so-called interstitial part (denoted IS). (Full potential denotes the fact that no shape approximation of the potential is done, either in the MT or in the IS.) In the IS every function is expanded with respect to plane waves. To describe the wave functions in the spheres the plane-wave basis is augmented by atomiclike functions. So a Bloch state in the LAPW formalism is given by

$$\psi_{\mathbf{k},j}(\mathbf{r}) = \sum_{\mathbf{G}} c_j(\mathbf{k}+\mathbf{G})\phi_{\mathbf{k}+\mathbf{G}}^{LAPW}(\mathbf{r}), \tag{15}$$

where the basis functions are defined as[40]

$$\phi_{\mathbf{k}+\mathbf{G}}^{LAPW}(\mathbf{r}) = \begin{cases} \dfrac{1}{\sqrt{\Omega}}e^{i(\mathbf{k}+\mathbf{G})\mathbf{r}}, & \mathbf{r} \in IS \\ \displaystyle\sum_{l,m}^{l_{max}} \{A_{l,m}(\mathbf{k}+\mathbf{G})u_l(r,\epsilon_l) + B_{l,m}(\mathbf{k}+\mathbf{G})\dot{u}_l(r,\epsilon_l)\}Y_{l,m}(\phi,\theta), & \mathbf{r} \in MT \end{cases}. \tag{16}$$

The division done in the LAPW method allows a good description of the rapidly oscillating wave functions inside the atomic spheres and the smoother wave functions in the IS. For Cu it has been shown that the band energies calculated within this method are in rather good agreement with results obtained by, e.g., photoemission experiments.[41] However, these experiments probe only the valence bands and provide therefore only a check of the theoretical results for the occupied bands. It is known that the LAPW method has problems

with (highly) excited states, partly because of the linearization of the energy with respect to a reference energy ϵ_l which typically lies within the valence bands. Equations (15) and (16) show the three fundamental numerical parameters which enter into the LAPW method, namely, the plane-wave cutoff, the maximum angular momentum l_{max} used in the MT, and the radius of the spheres R_{MT}. In order to check the stability of the unoccupied bands we varied these parameters.

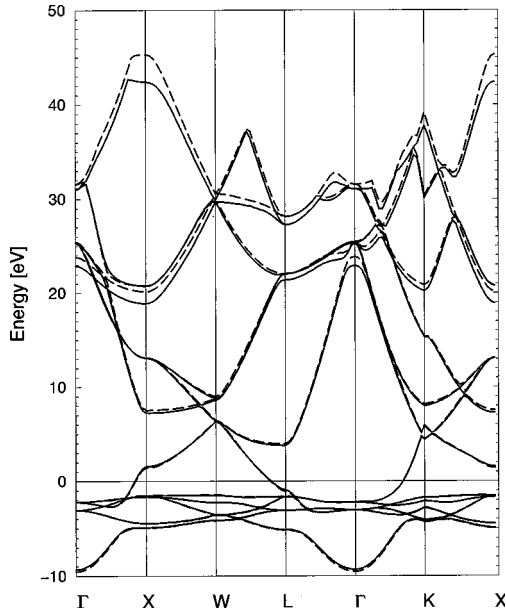The maximum l value is very uncritical. By default

FIG. 3. The band structure of Cu calculated using the LAPW basis set (solid line) and a plane-wave code (dashed line). The Fermi energy is set to zero. Up to about 25 eV the two band structures compare very well. Above this energy the LAPW band structure is not converged (see main text).

WIEN95 uses $l_{max}=10$, however, we found $l_{max}=8$ to be fully sufficient. There was no impact on either the unoccupied or the occupied bands. The cutoff was varied between 11 and 16 Ryd and the atomic sphere radius between 2.0 and 2.4 bohr. The occupied bands and the unoccupied bands up to about 20 eV above the Fermi energy were not affected by these variations. Higher lying bands, however, were strongly affected. We were not able to converge to a stable band structure for band energies above 20 eV. Even introducing extra local orbitals with energy parameters within the conduction band[42] did not improve on this situation although the linearization error should become smaller this way.

We also calculated the ground state of Cu using a plane-wave basis. Plane waves form a complete basis so any function can in principle be expanded with respect to this basis. However, it is not obvious that the band structure of the noble metal Cu can be obtained in this way, because the number of needed plane waves has to be kept at a level which does not make the calculation impossible. To calculate the band structure of Cu we used the program fhi96md.[36] The interaction between the ions and the electrons was described by a norm-conserving pseudopotential in the separable form of Kleinman and Bylander.[43] We used a soft Troullier-Martins pseudopotential.[44,45] We found that using a plane-wave cutoff of 60 Ryd is enough to converge the occupied bandwidth to within 0.2%.

Figure 3 shows a comparison of the band structures obtained with the two methods. Besides a small difference at the Γ point which results in a difference of 0.25 eV in the occupied bandwidth the agreement in the valence band is perfect. Above the Fermi level the differences between the two results increase. Above 40 eV there are differences up to 5 eV. These differences are due to the nonstable LAPW bands. The unoccupied bands obtained with the plane-wave calculation are converged.
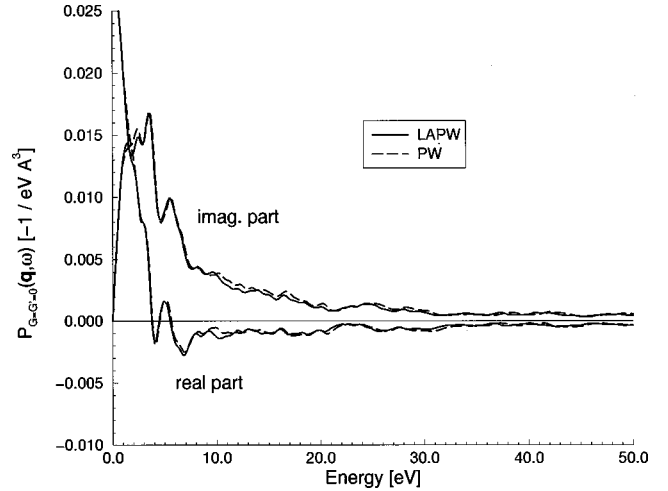

FIG. 4. The figure shows the polarizability $P_{G,G'}(\mathbf{q},\omega)$ of Cu calculated for a small wave vector $[\mathbf{q}=2\pi/a_0(-1/6,1/6,-1/6)]$ on the real frequency axis using a plane-wave basis set with an energy cutoff of 60 Ryd (dashed line) and a LAPW basis set (solid line). In the LAPW calculation the following parameters were used: $l_{max}=8$, $R_{MT}=2.4$ bohr., cutoff of 11 Ryd.

In both cases we used the exchange-correlation potential as obtained by Ceperley and Alder.[46] In WIEN95 the parametrization of Perdew and Wang[47] is used whereas the FHI code uses the parametrization of Perdew and Zunger.[48] It is unlikely that the difference in the occupied bandwidth is due to the different parametrizations.

The difference is also not caused by the different treatment of relativistic effects in the two programs. In the WIEN95 program the electronic structure inside the atomic spheres is calculated by solving the scalar-relativistic Schrödinger equation. In fhi96md relativistic effects enter via the pseudopotential. However, in both cases relativistic effects can be completely neglected by solving only the nonrelativistic Schrödinger equation. In both methods this resulted in a decrease of the occupied bandwidth, keeping the difference of 0.25 eV constant.

The FP-LAPW method is an all-electron calculation which means that in each iteration the electronic configuration of the core electrons is relaxed. In other words, the core electrons are allowed to interact dynamically with the valence electrons. In the kind of pseudopotential calculation presented here, by construction a so-called frozen-core approximation is used.[49] It might be possible that the resulting difference in the electronic structure of the core affects the lowest lying bands.

A comparison of the two band structures gives only information about the KS eigenvalues. For the many-body calculation we also need the wave functions. In order to test the agreement of the wave functions obtained within the two methods we calculated the polarizability of Cu using an expansion of the wave functions with respect to plane waves and LAPWs, respectively. In Fig. 4 the Fourier transform of the polarizability Eq. (11), $P_{G,G'}(\mathbf{q},\omega)$, for a small wave vector and $\mathbf{G}=\mathbf{G'}=0$ is shown. The solid line denotes the polarizability as obtained using the LAPW expansion of the wave functions with $l_{max}=8$, $R_{MT}=2.4$ bohr, and a cutoff of 11 Ryd. The dashed line corresponds to a plane-wave calculation using 22 bands and a cutoff of 60 Ryd. There are only
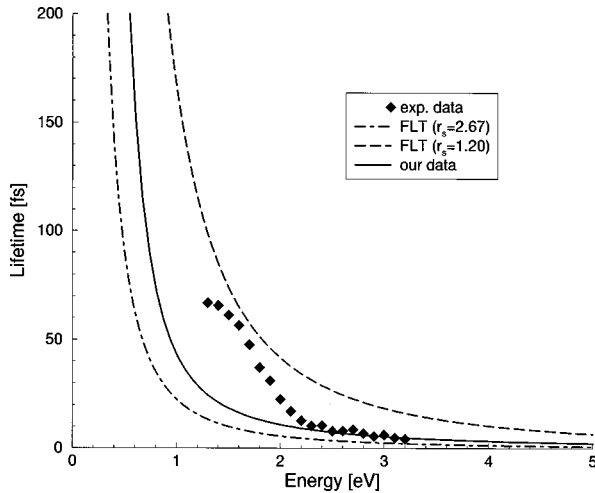
FIG. 5. The lifetime of excited electrons in Cu in the (110) direction. The solid line is the (in three dimensions) interpolated lifetime within the SIA. The dot-dashed line is the result of FLT using $r_s = 2.67$, the dashed line the one for $r_s = 1.20$. The diamonds are the measured lifetimes (Ref. 6). The energy is measured from the Fermi energy.

small differences between the two quantities; in the low frequency regime there is a difference around 2 eV. For larger frequencies ($\hbar\omega \gtrsim 10$ eV) the curves differ mildly. This is understandable from the differences in the band structure. We also compared the polarizabilities for larger wave vectors. Here the agreement becomes slightly worse.

B. Lifetime of excited states

The inputs for the calculation of the self-energy [Eq. (8)] are the LDA Green's function Eq. (6) which depends only on the LDA eigenvalues and the polarizability Eq. (11) which enters via the shielded potential. The results presented in Sec. IV A show that both quantities can be calculated equally precisely using a plane-wave or a LAPW basis set, respectively. We can therefore perform the many-body calculation using a plane-wave basis set. The calculation was done using 30 bands and a Monkhorst-Pack mesh[50] with 29 **k** points in the irreducible wedge of the Brillouin zone. As in the case of the transition metal Ni[17] this is sufficient.

As in the case of Al it is important to know which frequency of the pump laser was used in the experiments. In their experiments the Petek group[6] used 3.1 eV to 3.2 eV and they detected only electrons which were in intermediate states up to 3 eV above the Fermi energy. The experiments were conducted along the (100), (110), and (111) direction. However, by inspecting the band structure of Cu (see Fig. 3) it is obvious that only the sp band in the (110) direction (Γ-K) can be populated by photons of this energy. Therefore the only meaningful comparison of our data with the experimental ones can be along this direction. Figure 5 shows the lifetime of excited electrons along the (110) direction. The solid line is the result of the present calculation. The dashed line is the result of Fermi liquid theory, Eq. (12). For Cu we used $r_s = 2.67$, which corresponds to only considering the 4s electrons (four electrons in the cubic unit cell). Taking into account also the 3d electrons (44 electrons in the cubic unit

cell) would result in $r_s = 1.20$. In this case the lifetimes would be considerably larger.[51]

The complete information comes from the sixth band which cuts the Fermi surface at about 60% of the distance Γ-K (see Fig. 3). Above 2 eV the theoretical result and the experimental result, respectively, agree rather well. Below 2 eV the experimental lifetime suddenly increases. This behavior cannot be explained within the framework of the GW approximation or with single-particle states. The sudden increase is possibly due to Auger processes which contribute to the measured lifetimes of transition and noble metals at small energies. Therefore the experimental data could be larger than theoretical results which consider only electron-electron interactions.

The theoretical curve resembles very much the Fermi liquid result. On first sight this might be surprising. However, the band which crosses the Fermi surface in the Γ-K direction is an sp band and therefore very jelliumlike. On the level of the SIA the impact of the real band structure is therefore just a shift to longer lifetimes.

V. CONCLUSIONS

We presented results for the lifetimes of hot electrons in the crystals Al and Cu calculated *ab initio* within the shielded interaction approximation.

The "simple" metal aluminum really behaves simply with respect to the lifetimes of the excited electrons. Our data, calculated within the shielded interaction approximation for the self-energy using no further approximation (e.g., for the dielectric function), can explain the experimental data very well. We were able to identify the bands and directions whose electrons contribute to the experimental results obtained from a polycrystalline sample. Along the W-L direction we could identify the opening of another decay channel due to a band crossing, a genuine band-structure effect which cannot be described by Fermi liquid theory. In this respect Al is by no means simple, confirming the conclusions of the Aeschlimann group.[37] We are even able to give a crude estimate for the lifetime due to transport.

In Cu the theoretical and experimental results along the (110) direction agree down to 2 eV. Below 2 eV processes which are beyond the SIA or a single-particle picture, respectively, seem to have a strong contribution to the measured lifetimes. Cu reveals, however, another mystery; in experiments one can measure lifetimes in the (111) direction for electrons in the energy range of 1 eV to 3 eV above the Fermi energy. In this energy range there are no band states. As has been discussed in Sec. IV B these results can also not be explained within the shielded interaction approximation. Copper offers a third unsolved puzzle; as already mentioned in the Introduction the measured lifetimes of excited Cu electrons in these two directions depend on the frequency of the pump laser. It seems that in Cu a particle-hole interaction between the hole in the d band and the electron in the excited band exists which cannot be described by the GW approximation. Clearly further studies are needed.

In both elements the problem of how to handle the influence of transport processes at an *ab initio* level exists. Cur

rently neither theoretical nor experimental data are available that go beyond simple models. More studies of this effect are needed. In our calculations we also neglected the problem of the surface. Especially image states should contribute to the experimental data. We are planning calculations which include image states.

From a technical point of view we showed that Cu can be treated in a plane-wave basis extension. Both the band structure as well as the polarizability can be reliably calculated using a plane-wave cutoff of just 60 Ryd. This is of great importance since the calculation of the self-energy is computationally very demanding.

[1] H. Petek and S. Ogawa, Prog. Surf. Sci. **56**, 239 (1997).

[2] T. Hertel, E. Knoesel, M. Wolf, and G. Ertl, Phys. Rev. Lett. **76**, 535 (1996).

[3] E. Knoesel, A. Hotzel, T. Hertel, M. Wolf, and G. Ertl, Surf. Sci. **368**, 76 (1996).

[4] M. Aeschlimann, M. Bauer, and S. Pawlik, Chem. Phys. **205**, 127 (1996).

[5] S. Pawlik, M. Bauer, and M. Aeschlimann, Surf. Sci. **377-379**, 206 (1997).

[6] S. Ogawa, H. Nagano, and H. Petek, Phys. Rev. B **55**, 10 869 (1997).

[7] E. Knoesel, A. Hotzel, and M. Wolf, Phys. Rev. B **57**, 12 812 (1998).

[8] J. J. Quinn and R. F. Ferrell, Phys. Rev. **112**, 812 (1958).

[9] J. J. Quinn, Phys. Rev. **126**, 1453 (1962).

[10] D. Pines and P. Nozières, *The Theory of Quantum Liquids* (Addison-Wesley Publishing Company, Reading, MA, 1988).

[11] W. Kohn and L. J. Sham, Phys. Rev. **140**, A1133 (1965).

[12] R. M. Dreizler and E. K. U. Gross, *Density Functional Theory* (Springer-Verlag, Berlin, 1990).

[13] P. Hohenberg and W. Kohn, Phys. Rev. **136**, B864 (1964).

[14] G. D. Mahan, *Many-Particle Physics* (Plenum, New York, 1990).

[15] L. Hedin and S. Lundqvist, in *Solid State Physics: Advances in Research and Applications*, edited by H. Ehrenreich, F. Seitz, and D. Turnbull (Academic Press, New York, 1969), Vol. 23.

[16] Many-body perturbation theory does not necessarily lead to complex quasiparticle energies. In the simple Hartree or Hartree-Fock approximation, for example, the quasiparticle energies are real.

[17] F. Aryasetiawan, Phys. Rev. B **46**, 13 051 (1992).

[18] W.-D. Schöne, J. M. Sullivan, J. M. Gaspar, and A. G. Eguiluz (unpublished).

[19] W.-D. Schöne and A. G. Eguiluz (unpublished).

[20] G. Baym and L. P. Kadanoff, Phys. Rev. **124**, 287 (1961).

[21] L. Hedin, Phys. Rev. **139**, A796 (1965).

[22] F. Aryasetiawan and O. Gunnarsson, Rep. Prog. Phys. **61**, 237 (1998).

[23] H. J. Vidberg and J. W. Serene, J. Low Temp. Phys. **29**, 179 (1977).

[24] G. A. Baker, *Essentials of Padé Approximants* (Academic Press, New York, 1975).

[25] W.-D. Schöne and A. G. Eguiluz, Phys. Rev. Lett. **81**, 1662 (1998).

[26] A. G. Eguiluz and W.-D. Schöne, Mol. Phys. **94**, 87 (1998).

[27] B. Holm and U. von Barth, Phys. Rev. B **57**, 2108 (1998).

[28] R. T. M. Ummels, P. A. Bobbert, and W. van Haeringen, Phys. Rev. B **57**, 11 962 (1998).

[29] B. Farid, Philos. Mag. B **76**, 145 (1997).

[30] M. S. Hybertsen and S. G. Louie, Phys. Rev. B **34**, 5390 (1986).

[31] M. Rohlfing, P. Krüger, and J. Pollmann, Phys. Rev. B **48**, 17 791 (1993).

[32] A. Fleszar and W. Hanke, Phys. Rev. B **56**, 10228 (1997).

[33] M. P. Surh, J. E. Northrup, and S. G. Louie, Phys. Rev. B **38**, 5976 (1988).

[34] L. Hedin, Int. J. Quantum Chem. **56**, 445 (1995).

[35] We used the fhi96md (Ref. 36) plane-wave code to calculate the ground state of Al.

[36] M. Bockstedte, A. Kley, J. Neugebauer, and M. Scheffler, Comput. Phys. Commun. **107**, 187 (1997).

[37] M. Bauer, S. Pawlik, and M. Aeschlimann, Proc. SPIE **3272**, 201 (1998).

[38] D. J. Singh, *Planewaves, Pseudopotentials and the LAPW Method* (Kluwer Academic Publishers, Boston, 1994).

[39] P. Blaha, K. Schwarz, P. Dufek, and R. Augustyn, WIEN95, Technical University of Vienna 1995. [Improved and updated Unix version of the original copyrighted WIEN code, which was published by P. Blaha, K. Schwarz, P. Sorantin, and S. B. Trickey, Comput. Phys. Commun. **59**, 399 (1990).]

[40] In actual implementations of the LAPW method, the basis functions in the spheres have an additional term (local orbitals) in order to avoid spurious eigenvalues (ghost bands) (Ref. 38).

[41] V. N. Strocov, R. Claessen, G. Nicolay, S. Hüfner, A. Kimura, A. Harasawa, S. Shin, A. Kakizaki, P. O. Nilsson, H. I. Starnberg, and P. Blaha, Phys. Rev. Lett. **81**, 4943 (1998). The measured energies for the sp bands and the calculated energies within the LAPW agree very well. The calculated d-band energies are 0.3 eV to 0.5 eV higher than those measured.

[42] This idea goes back to discussions in the group of A. G. Eguiluz with D. Singh.

[43] L. Kleinman and D. M. Bylander, Phys. Rev. Lett. **48**, 1425 (1992).

[44] N. Troullier and J. L. Martins, Phys. Rev. B **43**, 1993 (1991).

[45] M. Fuchs and M. Scheffler, Comput. Phys. Commun. **119**, 67 (1999).

[46] D. M. Ceperley and B. J. Alder, Phys. Rev. Lett. **45**, 566 (1980).

[47] J. P. Perdew and Y. Wang, Phys. Rev. B **45**, 13 244 (1992).

[48] J. P. Perdew and A. Zunger, Phys. Rev. B **23**, 5048 (1981).

[49] Pseudopotential calculations do not use by definition the frozen-core approximation. In quantum chemical calculations, very often polarizable core potentials are used; see, e.g., V. Bonačić-Koutecký, P. Fantucci, and J. Koutecký, J. Chem. Phys. **93**, 3802 (1990).

[50] H. J. Monkhorst and J. D. Pack, Phys. Rev. B **13**, 5188 (1976).

[51] For non-NFE metals the concept of an electronic Wigner-Seitz radius is at least dubious. The r_s values quoted in the main text were obtained from the average electronic density of the non-core electrons. For Cu this leads to the two possibilities. There is one more possibility; r_s could be calculated from the Fermi energy as obtained from an *ab initio* calculation, $r_s = (9\pi/4)^{1/3}\sqrt{\hbar^2/2mE_F}$.